Supporting Information

Sucralose with Bifunctional Groups as a Functional Additive Enhancing Interfacial Stability of Zinc Metal Anode *via* Interfacial Molecular Chemistry Regulation

Huan Liu[a], Zijun Xin[a], Bin Cao[a,] *, Di Zhang[b], Jie Lu[a], Yiwen Zhang[a], Zhijing Xu[a], Hongjuan Lai[a], Mengjiao Du[a], Zirong Guo[a]

[a] *College of Materials Science and Engineering, Xi'an University of Science and Technology, Xi'an 710054, China*

[b] *State Key Laboratory of Space Power Sources, Shanghai Institute of Space Power-Sources, Shanghai 200245, China*

Experimental Section

Preparation of Electrolyte and MVO. the Sul/$ZnSO_4$ electrolyte was prepared by dissolving pure sucralose (0.1M) into a 2 M $ZnSO_4$ solution at room temperature. $ZnSO_4 \cdot 7H_2O$ was purchased from Macklin, while Sucralose (99.5%) was purchased from Aladdin. For the synthesis of MVO, 0.2 g NH_4VO_3, 0.2 g $Mn(CH_3COO)_2$ and 3.0 g $C_{12}H_{25}SO_4Na$ were dispersed into 60 mL deionized H_2O under stirring at 60°C for 30 mins, then the solution was transferred into a Teflon-lined stainless-steel autoclave. The sealed autoclave was heated to 180°C for 24 h. Finally, the MnVO sample was collected by centrifugation and washed with water and ethanol for several times. The sample was dried at 60°C in a vacuum oven for 12 h.

Synthesis of cathode materials and assembly of Zn||MVO full cells. The cathode material was prepared by blending MVO with conductive carbon black and polyvinylidene fluoride (PVDF) at a weight ratio of 8:1:1. The mixture was dissolved in an appropriate amount of N-methyl-2-pyrrolidone (NMP) to form a homogeneous slurry. This slurry was then coated onto stainless steel and dried in a vacuum oven at 80 °C overnight. The mass loading of the cathode active

materials was approximately 1.5 to 2.0 mg cm^{-2}. 2 M $ZnSO_4$ or Sul/$ZnSO_4$ were utilized as the electrolyte. Full cells were assembled in coin cells under an air atmosphere, with zinc foil serving as the anode and a glass fiber membrane as the separator.

In the case of MVO//Zn full pouch cells, the anodes were Zn plates, while the cathode material was MVO. These components were separated by a glass fiber separator, and a single-layer electrode was used in the pouch cell. The electrolyte employed in this configuration was 60 μL of Sul/$ZnSO_4$ solution. The Zn foil and the cathode were cut into dimensions of 3.2 cm × 3.2 cm, while the separator was cut into dimensions of 3.6 cm ×3.6 cm. The transparent plastic film was approximately 4 cm × 4 cm.

Material Characterization. The micromorphology of Zn deposition was examined using a scanning electron microscope (FESEM, Hitachi S-4800), while the crystal structure of Zn deposits on the electrodes was analyzed by X-ray diffraction (XRD) with Cu Kα radiation and a scan rate of 5°/min (XRD, Bruker D8 Advance Diffractometer). The Zn deposition process was visualized through in situ images captured using a YUESCOPE (YM710R) optical microscope, utilizing Zn plates with current density of 10 mA cm^{-2} and duration time of 1 h. Electrode wettability was assessed with a POWEREACH JC2000DM contact angle tester using a 10 μL electrolyte droplet, and Fourier-transform infrared spectroscopy (FLIR E4, Picotech, UK) was employed for further characterization. Surface temperatures of the samples were recorded with a TC-08 thermocouple thermometer (Picotech, UK), and thermal profiles were documented with a FLIR E4 thermographic camera. Additionally, Raman spectroscopy (HORIBA Scientific LabRAM HR Evolution) was conducted for additional analysis. White light interferometry (WLI) characterization was performed on Atometrics-EX230.

Electrochemical Measurements. Two pieces of symmetric Zn foils were used as the two electrodes for the Zn||Zn symmetric cell. 70 μL of different electrolytes (2 M $ZnSO_4$, 2 M $ZnSO_4$ with 0.1M Sucralose) were dispensed into CR2025-type coin cells, with a piece of glass fiber serving as a separator. In one set-up, one piece of the Zn foil in the Zn||Zn cells was replaced with a Cu foil, while keeping the other experimental conditions unchanged. Electrochemical characterization of Cu||Zn and Zn||Zn cells with a glass fiber separator was conducted using 2025-type coin cells. The cells were galvanostatically charged/discharged at various current densities using Neware batteries testing system (CT-4008T-5V50mA-164, Shenzhen, China). In the three-electrode system, a saturated calomel electrode (SCE) served as the reference electrode, and a Pt foil electrode was employed as the counter electrode for the tests. Electrochemical impedance spectroscopy (EIS), Tafel, and linear sweep voltammetry

(LSV) curves were measured using an DH7000 electrochemical workstation (Jiangsu Donghua Testing Technology Co., Ltd.).

Theoretical calculations. The generalized gradient approximation (GGA) was employed along with the Perdew-Burke-Ernzerhof (PBE) functional. The core wavefunctions were described using the projector-augmented wave (PAW) method, while valence wavefunctions were represented as a linear combination of plane waves with a cut-off energy of 500 eV. Throughout the geometric optimization process, the total energy converged to 10-5 eV, and the Hellmann-Feynman force experienced by each atom post-relaxation was below 0.02 eVÅ-1. We ensured a vacuum space of over 20 Å between consecutive sheets to mitigate interaction effects. The climbing image nudged elastic band (NEB) approach was employed to identify transition states and determine activation barriers. The adsorption energy was calculated using the formula: E(ads) = E (Zn + Surface) - E(Surface) - E(Zn).

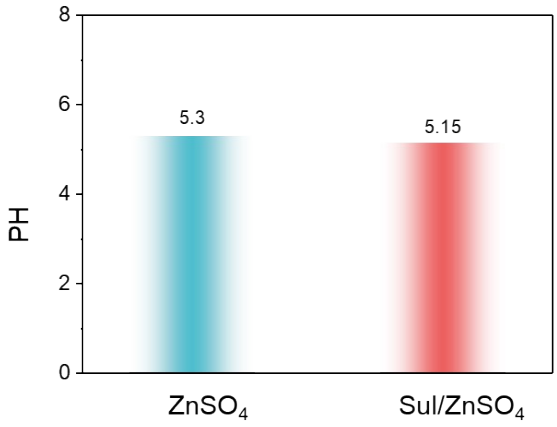

Figure S1. pH of electrolytes with/without Sul additive.

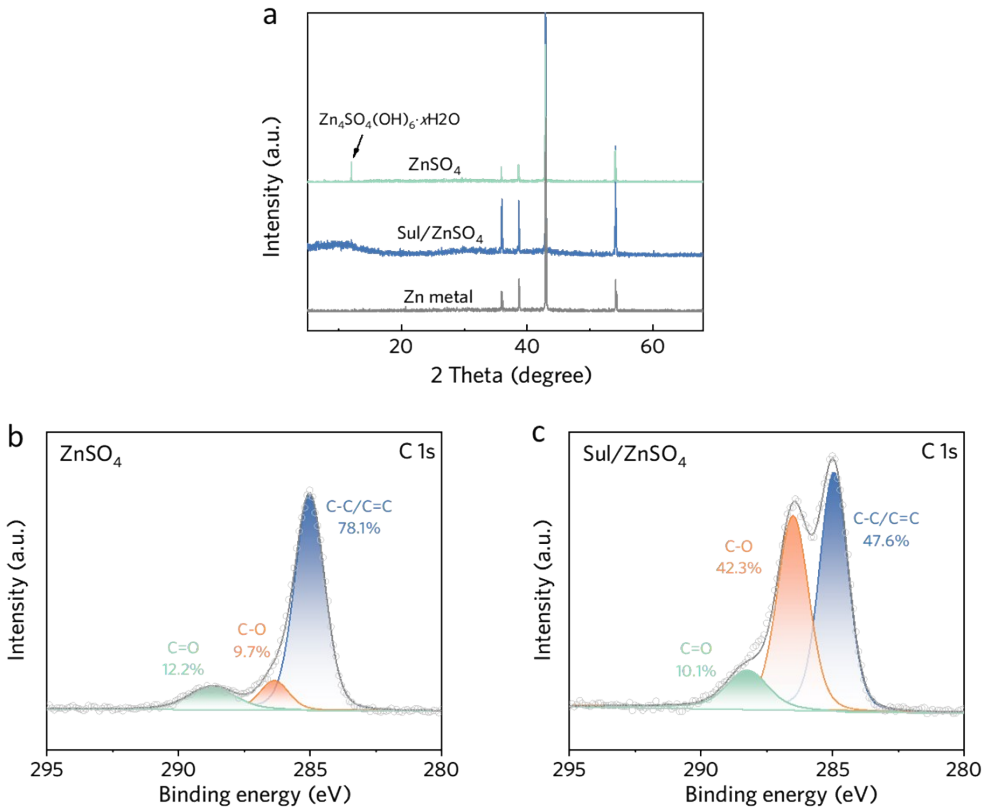

Figure S2. (a) The XRD pattern of zinc electrodes after immersion in $ZnSO_4$ and Sul/$ZnSO_4$ electrolytes. C 1s XPS spectra of zinc electrodes after immersion in $ZnSO_4$ (b) and Sul/$ZnSO_4$ electrolytes (c).

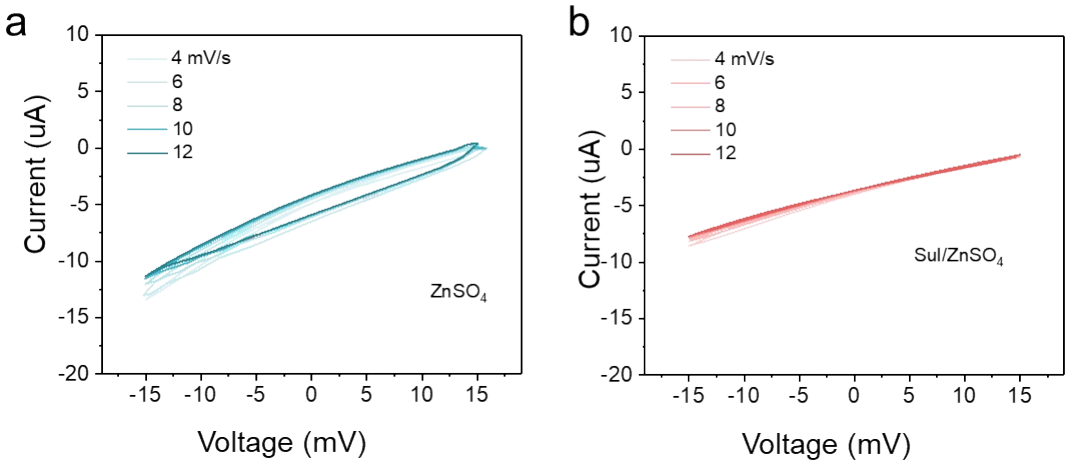

Figure S3. Electric double layer capacitance measurements for Zn substrates in (a) $ZnSO_4$ and (b) Sul/$ZnSO_4$ electrolytes. Cyclic voltammograms of Zn-Zn symmetric coin cells recorded within a voltage range of -15 mV to 15 mV under different scanning rates.

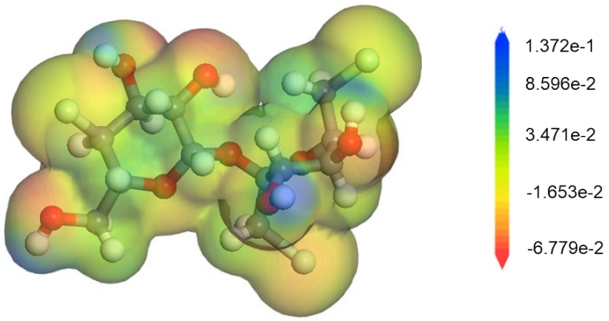

Figure S4. Electrostatic potential mapping of sucralose reveals two potential Zn adsorption sites.

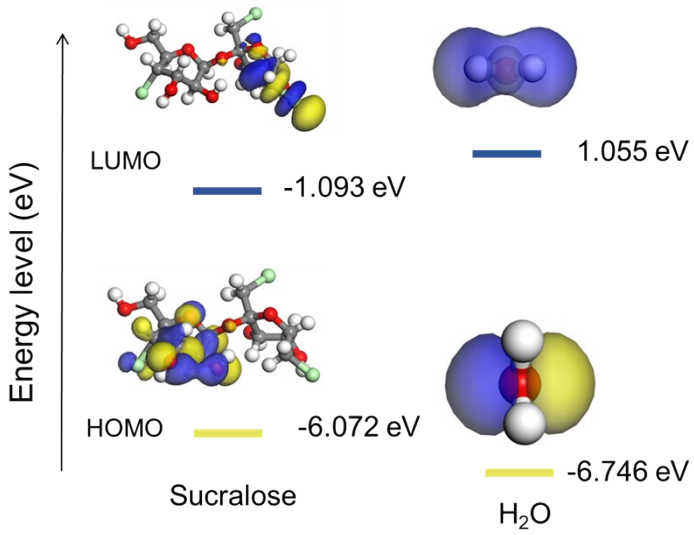

Figure S5. Isoelectronic density surfaces for the LUMO and HOMO of Sucralose (left) and water molecules (right).

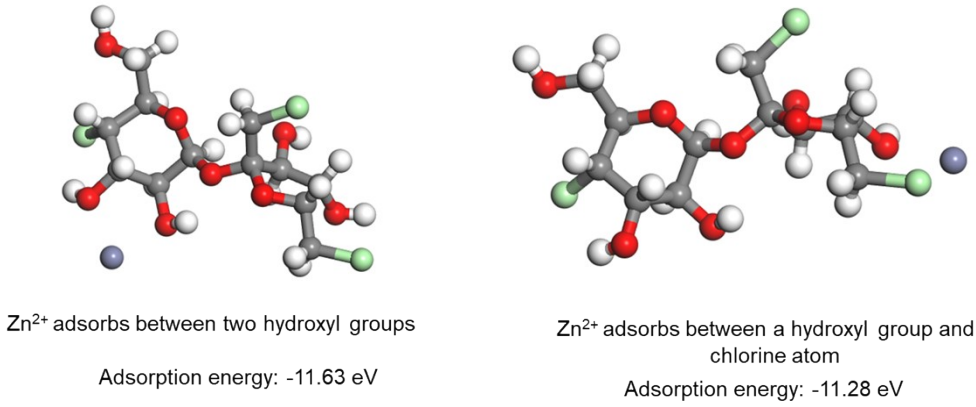

Figure S6. DFT-calculated adsorption energies for different Sucralose-Zn^{2+} species interactions.

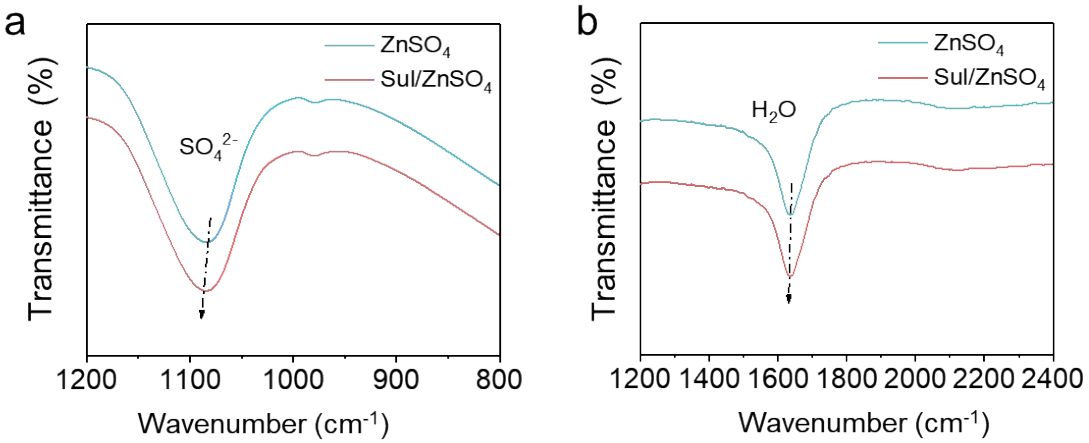

Figure S7. FTIR spectra comparing with and without sucralose additive.

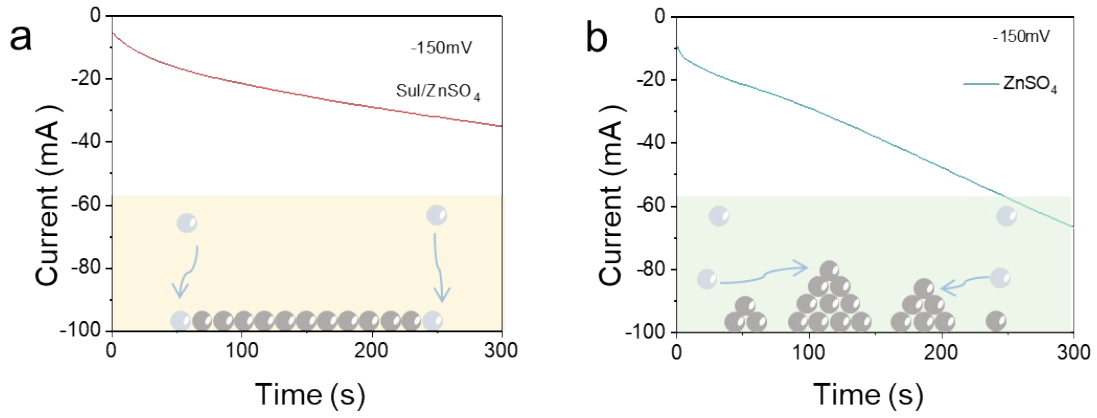

Figure S8. The chronoamperometry curves of the Zn plate tested at a fixed overpotential of -150 mV for (a) Sul/$ZnSO_4$ and (b) $ZnSO_4$.

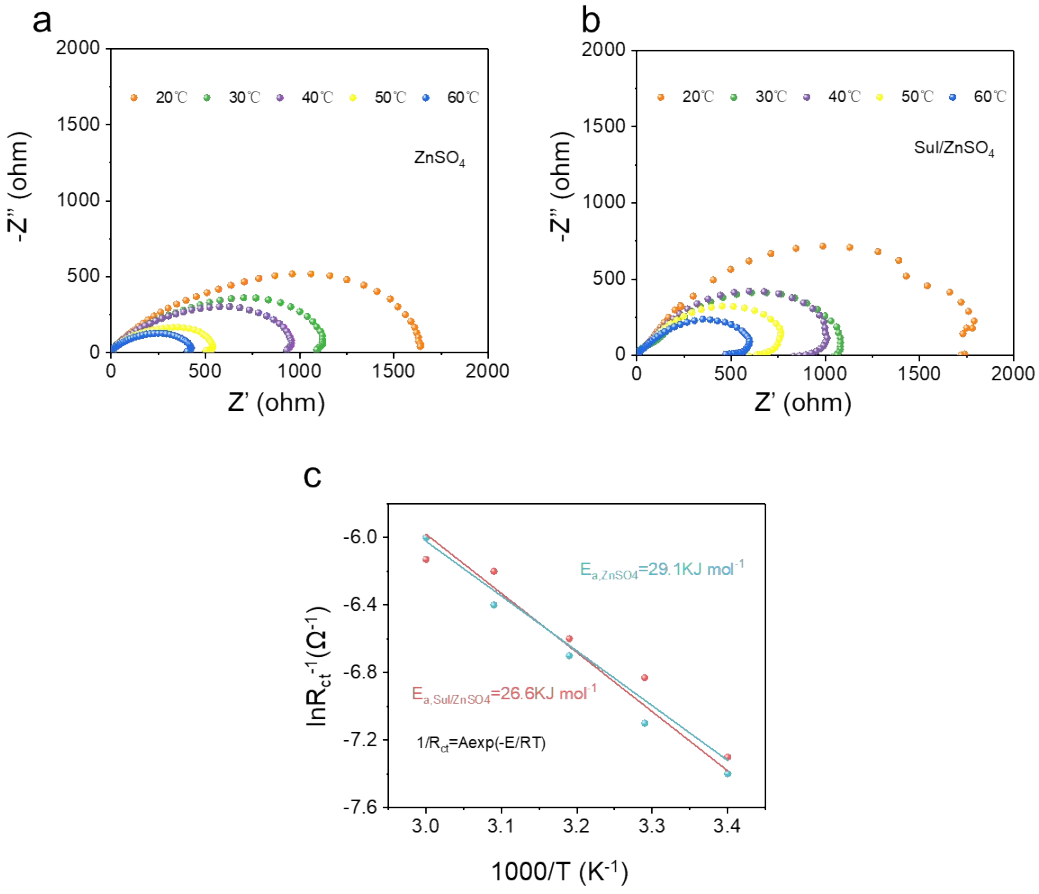

Figure S9. Nyquist plots at different temperatures for (a) $ZnSO_4$ and (b) Sul/$ZnSO_4$. (c) Corresponding Arrhenius curves and comparison of activation energies.

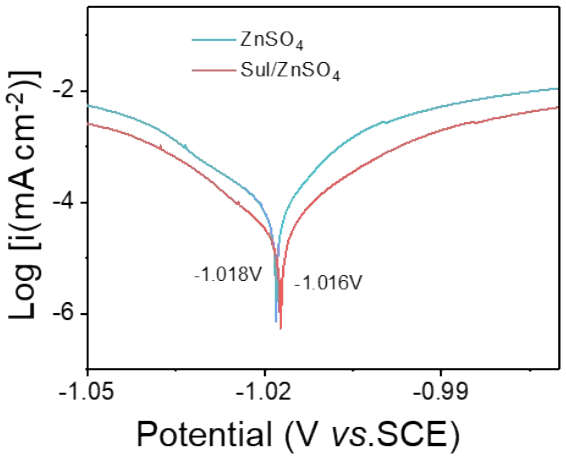

Figure S10. The Tafel plots were measured at 1.0 mV s^{-1}.

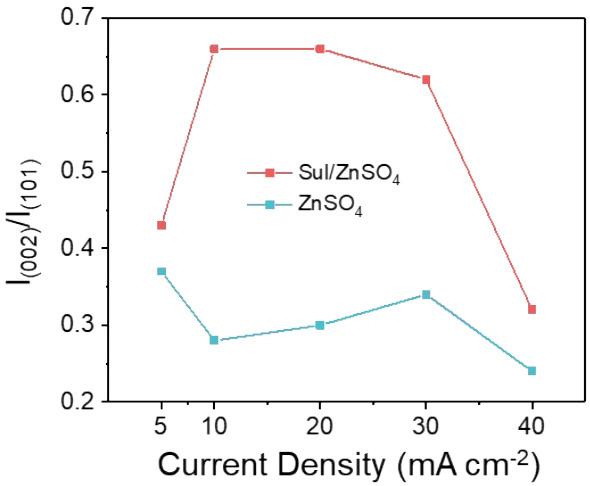

Figure S11. Plots of the $I_{(002)}/I_{(101)}$ ratio versus the current density.

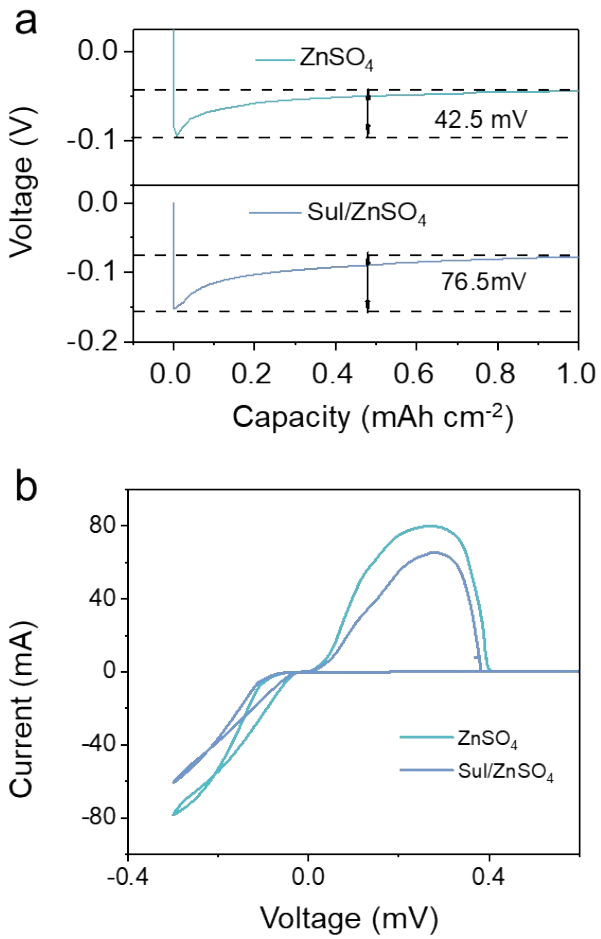

Figure S12. (a) The first discharge profile; (b) CV curves of the Zn//Cu cell with and without the addition of sucralose in the electrolyte.

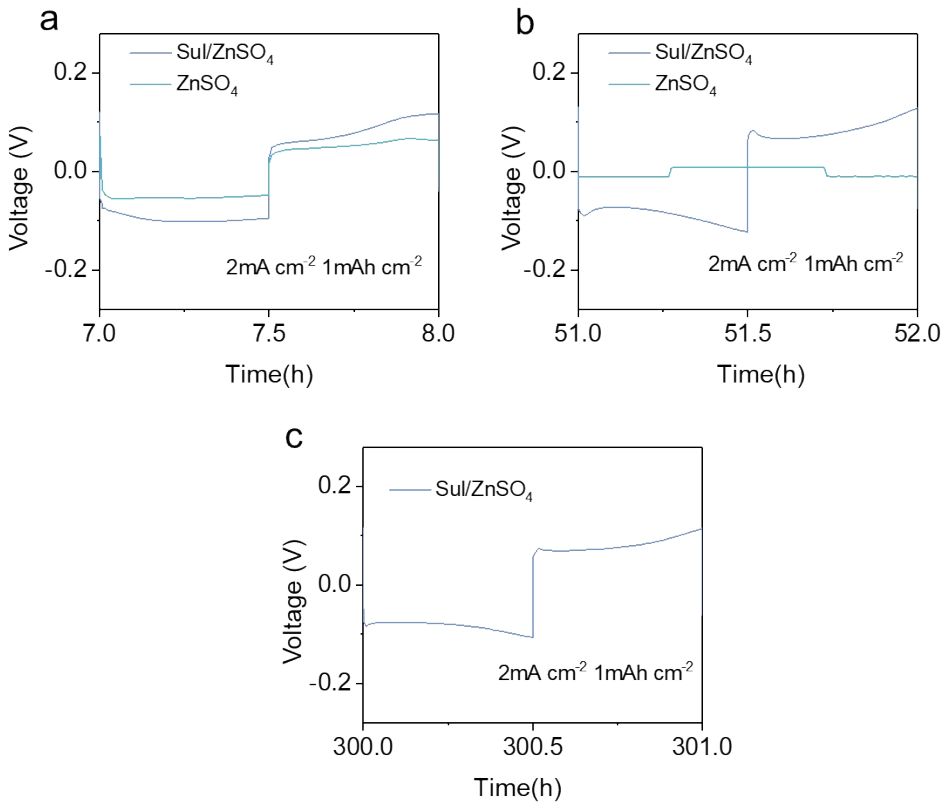

Figure S13. The magnified voltage profiles for selected times at 2 mA cm^{-2} and 1 mAh cm^{-2}.

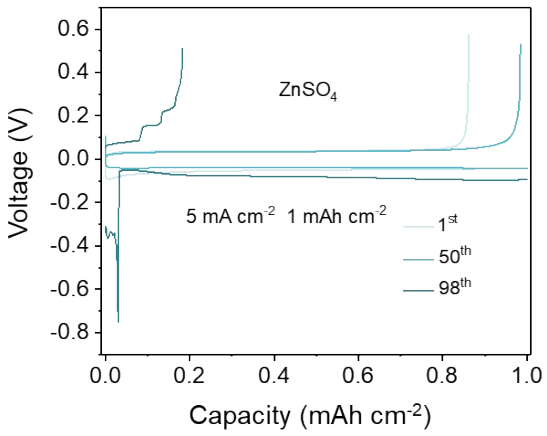

Figure S14. The corresponding voltage profiles at different cycles with $ZnSO_4$ electrolytes.

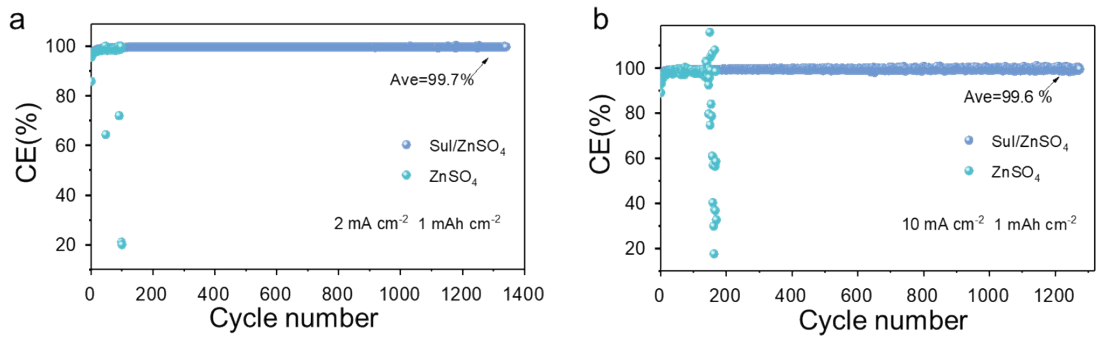

Figure S15. CE measurements of Zn//Cu cells (a) at 2 mA cm^{-2}/1 mAh cm^{-2} and (b) 10 mA cm^{-2}/ 1 mAh cm^{-2}.

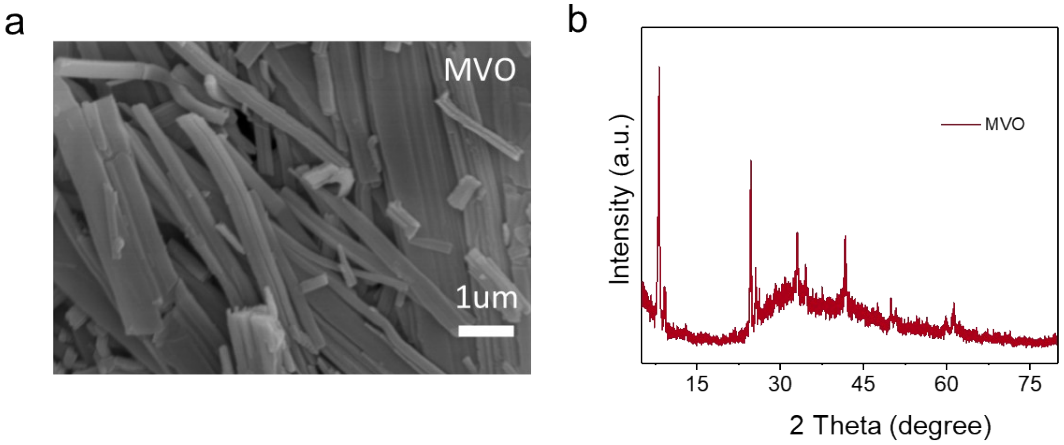

Figure S16. (a) SEM and (b) XRD of MVO.

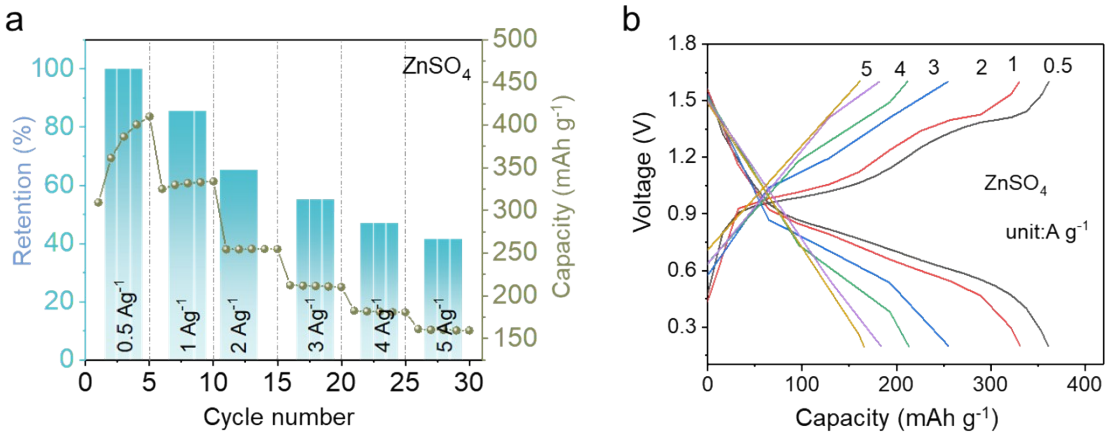

Figure S17. (a) Rate performances of Zn//MVO full cells using $ZnSO_4$ electrolytes and (b) corresponding voltage profiles.

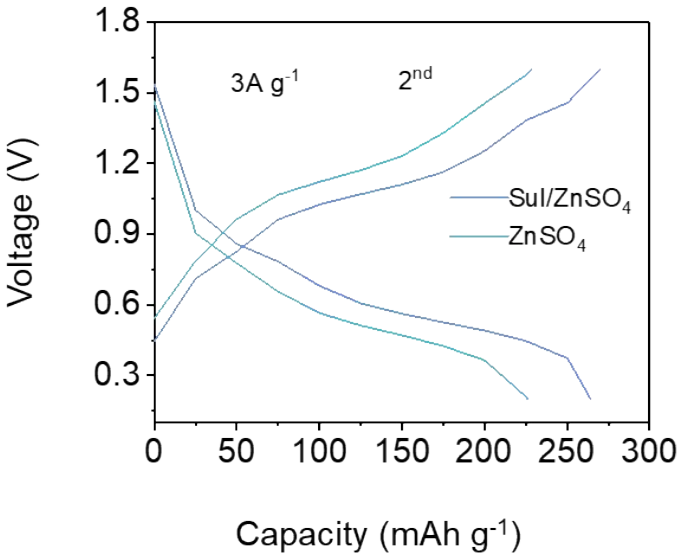

Figure S18. The voltage profiles of full cells in electrolytes with/without SuI additive at same cycles.

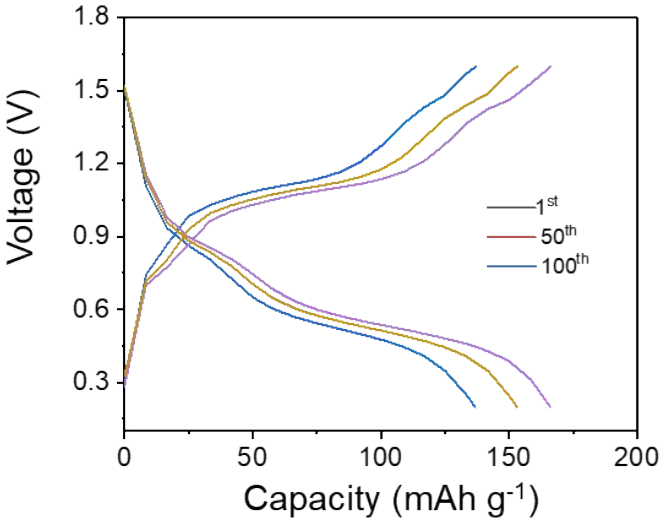

Figure S19. The voltage profiles of full cell in Sul/$ZnSO_4$ electrolyte at different cycles.